17

Atomic Force Microscopy of Interfacial Monomolecular Films of Pulmonary Surfactant

Kaushik Nag, Robert R. Harbottle, Amiyo K. Panda, and Nils O. Petersen

1. Introduction

Pulmonary surfactant (PS) is a lipid protein complex secreted at the terminal airways of the lung. The material is secreted as lipid rich multilamellate bodies, which transforms into lipid–protein tubules, planar bilayers, and monomolecular films at the alveolar air–aqueous interface ***(1,2)***. The films reduce the surface tension of the interface and prevents lung collapse during end expiration ***(3)***. PS layers also act as a protective barrier against inhaled particles and bacteria and keeps the upper airways or bronchioles open during respiration ***(3)***. Dysfunction of PS has been implicated in various lung diseases, such as asthma, acute respiratory distress syndrome, cystic fibrosis, and pneumonia ***(4)***. The composition of PS is conserved in most air-breathing species; however, its high content of saturated phosphatidylcholine (PC) and phosphatidylglycerol (PG) is unique compared with other secretory materials and cell membranes, which lack these phospholipids ***(1,5)***. Specifically, PS contains significant amounts of dipalmitoylphosphatidylcholine (DPPC), palmitoyl-oleyl-PC (POPC) and PG (POPG), cholesterol, and small amounts (10%) of surfactant proteins SP-A, SP-B, SP-C, and SP-D ***(1)***. It is not clear to date how this lipid–protein complex functions by forming alveolar films or barrier *in situ* because such fragile and dynamic films are difficult to preserve for traditional electron microscopy ***(2,3)***. In vitro studies have focused on model lipid–protein films of PS and also by extracting the material out of lungs and studying interfacial properties of surface tension of such material using Langmuir and other surface balances ***(6–8)***. We have taken an approach of studying such surfactant films from lungs of normal as well as those in dis-

From: *Methods in Molecular Biology, vol. 242: Atomic Force Microscopy: Biomedical Methods and Applications*
Edited by: P. C. Braga and D. Ricci © Humana Press Inc., Totowa, NJ

eased states using a combination of fluorescence and atomic force microscopy (AFM) ***(9)***.

Monolayer films have also become a standard model for studying lipid–protein interactions and associations in biological membranes ***(10)***. Models of interactions of enzymes with lipid membranes, two-dimensional crystallization of proteins, the binding kinetics of soluble proteins with a substrate, and biosensor developments have also been studied using monolayer films ***(10)***. Lipid films undergo a lateral phase separation from gas to fluid to gel-like phase with increasing surface packing density driven by increasing lateral pressure ***(11)***. The inherent changes of packing the lipid in a film undergoing lateral phase separation allows for the imaging of the structures and processes associated with formation of gas, fluid, gel, and solid domains, as well as supramolecular aggregates ***(10)***. The domain structures can be imaged using fluorescence and Brewster angle microscopy directly at the air–water interface. By depositing them on solid substrate using Langmuir–Blodgett technique***(12)***, it is also possible to image them by AFM ***(12,13)***. The contrast in AFM image of these domains arises from differences in the molecular tilt and density of the lipids in the separate phases. Typical vertical height profiles, or topography, of films deposited on an atomically flat surface vary on the nanometer level ***(14–17)***. Thus AFM at an atomic resolution show fatty acid chains and lattice spacing of single molecules of DPPC within films ***(17)***. These and other AFM studies have demonstrated that mono-molecular films can be used to study the molecular structure–function properties of PS and biomembrane components ***(13,16)***. This chapter focuses on the methodology for preparation and imaging monolayer films using AFM to study lung surfactant and suggests a relatively simple method to study molecular organization and disorganization (during dysfunction ***(18)***) of lipid–protein systems at an interface.

AFM uses a sharp tip to scan the surface of materials, which are rough at the nanometer or atomic level. Because of the interactions and deflections of the tip with the corrugated surface, real-time imaging and physical properties (friction) of such surfaces are possible in air and in liquid ***(12,13)***. However, AFM imaging of lipid films with phase transitory structures is only possible in air because the amphipathic lipids phase transition or domain formation arise from the differences in tilt of the hydrocarbon chains in air. This phase heterogeneity of packing is not observed in bilayers or monolayers, from the polar headgroups in water ***(11,15)***. However, protein–lipid interactions, binding, and crystallization processes of the proteins are better imaged in AFM in the polar head-group region because in a number of situations such processes occur in a polar environment ***(12,13)***. It is also possible to image soluble or hydrophobic proteins inserted into lipid films by AFM in air because such proteins interfere

with the lipid packing ***(19)***. In case of dysfunction of surfactant as in respiratory disease, such as acute respiratory distress syndrome, leaked plasma proteins can enter the films from the lung aqueous interface and disrupt the surface activity of PS ***(4,18)***. We have used surfactant from a bovine source (bovine lipid extract surfactant, or BLES) and surfactant from a normal and ventilation injured rat lungs (dysfunctional surfactant), and studied them in planar films using AFM. The methods to form and study such films by AFM, and specific information about lipid packing of surfactant at an air–water interface obtained using AFM are discussed.

2. Materials

1. Synthetic phospholipids of high purity, such as DPPC, POPC, and a fluorescent probe 1-palmitoyl, 2-nitrobenzo-dioxo-dodecanoly phosphatidylcholine (NBD-PC) are available from Avanti Polar Lipids (Birmingham, AB) ***(6)***. These lipids are required to measure and standardize the surface pressure-area isotherms of films and to image structure formation as a model for surfactant ***(8,14,19)***.
2. Commercial clinical preparations of pulmonary surfactant, such as BLES (BLES Pharmaceuticals, London, Ontario, Canada), or calf lipid surfactant extract (ONY Inc., Amherst, NY) are available. These surfactants are used mainly in clinical trials and are commercially available as a pharmaceutical product for research. They contain most of the lipid and hydrophobic protein components of natural surfactant extracted from animal lungs, except the water soluble proteins SP-A and SP-D ***(1)***. We have also obtained surfactant from ventilation injured rat lungs ***(18)***, however a simple model for such surfactant can be prepared from a clinical source or similar materials can made from 10:1 wt/wt of (lipid/protein ratio) of BLES:serum protein mixtures.
3. High-purity organic solvents (99.1% high-performance liquid chromatography grade) chloroform and methanol are needed for solubilizing surfactant for film formation. Also small volumes of fluorescent probe NBD-PC in 2-5 micro liter (μL) of methanol can be directly added to the emulsion of the surfactant to form adsorbed films at the air-water interface. We have applied this method in conjunction with solvent spreading, and find both techniques yield similar film microstructures in the compressed films ***(19)***.
4. Doubly glass distilled and deionized water of resistivity above 18 MΩ (megaohms) is required. The second distillation in this case can be performed using dilute $KMnO_4$ to remove mainly organic surface-active contaminants. It is absolutely necessary for reproducible results (**Note 1**). Surface tension of such clean water can be measured using the surface balance and should be close 72 mN/m at 23 ± 1°C (*see* **Subheading 3.11.**).
5. Cleaned glass and mica slides are required for film deposition for AFM imaging. The glass slides can be 1 cm diameter coverslips that can fit the AFM magnetic base or freshly cleaved mica of the same dimension. In case of the glass cover slips, they need to be washed first with chloroform:methanol (2:1, vol/vol) and then rinsed in chromo-sulphuric acid and doubly distilled water. Such mica and

glass are to be dried in air and preserved in covered Petri dish and used directly during film deposition to avoid contaminants in the surrounding air from coming in contact with the surface on which the film is to be deposited.

6. A dedicated Langmuir–Wilhelmy surface balance with fluorescence imaging attachments was used in all experiments. Design and construction of such a balance is discussed in details elsewhere ***(20)***. Ours is a commercially available model (Kibron Scientific, Helsinki, Finland).
7. Scanning probe or an AFM with Silicon Nitride probes is required for film imaging ***(2,9)***. In our studies we use a DI Nanoscope IIIa (Digital Instrument, Santa Barbara, CA) scanning probe microscope with contact, tapping and tunneling mode abilities. However, other commercially available AFMs also can be used with minor alterations of the methods discussed below for films imaging. Gold-coated SiN_3 cantilevers (Wafer-113-135-22 Nanoprobe SPM tips, DI) with nominal spring constants of 0.06 or 0.38 N/m was used for contact and lateral force (friction) imaging with either a J (normal resolution) or E (high resolution) scanner.

3. Methods

3.1. Film Preparation

1. The Langmuir trough is filled with doubly distilled water, and the surface activity of this water is measured with a Wilhelmy dipping plate ***(20)***.
2. The open water interface is compressed from maximal to minimal surface area, and any surface tension drop is monitored below 72 mN/m (milli Newton/ meter) or that of a clean air-water interface. Using a suction apparatus with a sharp nozzle (Pasteur pipet), the surface contaminants are removed until the surface pressure reaches 0 mN/m or surface tension reaches 72 mN/m (*see* **Note 1**).
3. DPPC dissolved in chloroform:methanol (3:1 vol/vol) is applied drop-wise on this clean water interface using a micro-calibrated Hamilton syringe (10–50 μL) to form the monomolecular film. A total of 20 nM of phospholipid is applied, if the surface area of the trough is close to 120 cm^2 to give an area per molecule of DPPC to be 100 $Å^2$.$molecule^{-1}$ ***(6,20)***. Lung surfactant or BLES films can also be formed using exactly the same technique except because BLES is a complex lipid mixture an arbitrary or average area per molecule is calculated based on the average molecular weight of the material of 750 Da. The fluid phospholipid POPC should also have similar area per molecule as those of BLES. In case of adsorbed films (**Subheading 2.3.**), similar amounts of the surfactant solution is injected from the syringe just below the air-water interface resulting in an initial surface pressure raised to 2 mN/m. Most Langmuir surface balance software allows for automatic calculations of such film area and details of specific calculations on surfactant films are discussed elsewhere ***(6,8)***.
4. The DPPC film is rapidly compressed and the surface pressure–area profile monitored (**Fig. 1**). The phospholipid undergoes a two-dimensional phase transition, and this is seen in the pressure-area isotherms as a broad plateau around 5-8 mN/m (**Fig. 1A**). If this plateau does not occur then either the surface has not been cleaned enough, or the solvent or phospholipids contains contaminants.

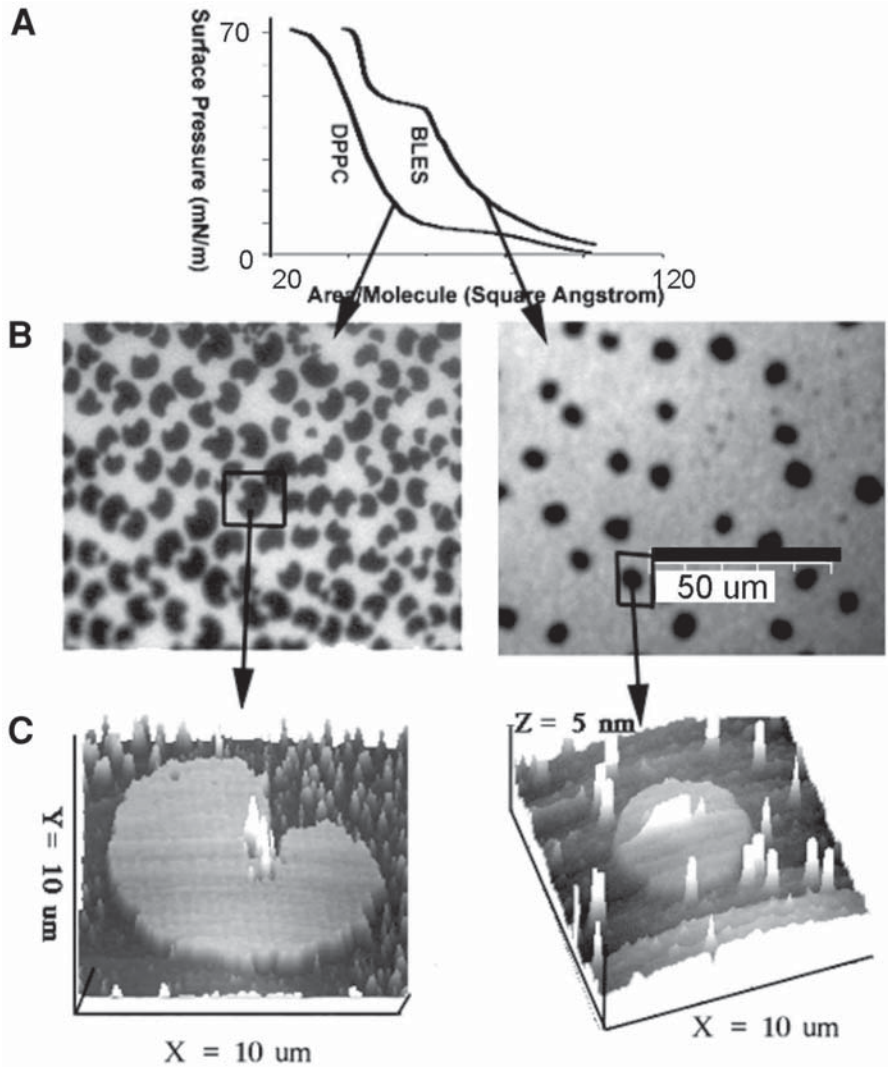

Fig. 1. Surface pressure–area isotherms of DPPC and BLES films **(A)** and typical fluorescence **(B)** and atomic force **(C)** microscope images of such films at the phase coexistence region of the isotherms (surface pressure of 16 mN/m). The plateau region of the DPPC isotherm in **(A)** suggests an expanded to condensed phase transition occurring at 4–8 mN/m. The plateau in BLES (at 45 mN/m) isotherm is possibly a higher order transition, considering that the fluid-gel transition occurs at lower pressures of 10–40 mN/m ***(6)***. The black regions in the fluorescence images **(B)** represent the gel or condensed phase and the lighter region the fluid or expanded phase, upon which the probe partitions. The gel regions have higher height than the surrounding fluid phase as seen in the deposited film shown in **(C)**, and this allows for topographical imaging of films via AFM.

5. BLES films will not show any plateau-like region below 45 mN/m (**Fig. 1A**), however a broad phase transition does occur between 5 and 45 mN/m. The BLES film isotherm would look similar to the one of POPC compressed at the same rate and initial area. This phase transition in BLES or DPPC films can be visually observed either by depositing the films and imaging them via AFM or using small amounts of fluorescent probe incorporated in the films and imaging them by fluorescence microscopy ***(20)***. Typical images taken from a DPPC and BLES films using fluorescence microscopy are shown in **Fig. 1B**. The black regions in the images are gel-phase domains coexisting with the homogeneously fluorescent fluid or bright regions.
6. Films are deposited on clean glass (**Subheading 2.5.**) or mica slides (*see* **Note 2**) by Blodgett deposition. The process requires a slow 0.2–10 $mm^2 \cdot s^{-1}$ up-stroke or vertically lifting of the slides from the subphase to air, termed as Blodgett deposition ***(14–16)***. The slides are originally placed into the subphase before spreading of the films from the solvent. The deposited films can be kept on a Petri dish with wet filter paper, for up to 2 days depending on the substrate of deposition. Films on glass substrates are more stable than mica, however other complications may arise using glass substrates (**Note 2**). Comparative AFM of the deposited films (from fluorescence imaging) showing single gel domains for DPPC and BLES are shown in **Fig. 1C**.

3.2. Film Imaging by AFM

1. Set the mode for imaging in the Nanoscope IIIa AFM to contact mode.
2. The glass or mica slide with the films are to be attached firmly to the magnetic disk or AFM base of the E (12 μm) or J (120 μm) scanner. Mount the disk onto the scanner head.
3. Attach the tip-cantilever to the metallic head of the AFM.
4. Adjust the laser to focus on the center of the tip. This is generally performed by observing the tip under an optical microscope or camera focused on the tip from above the scanner. General methodology for this is available in the manual supplied with the instrument.
5. Turn on the software program to online mode, and allow the tip to come in contact with the films surface. Set initial scan parameters to Integral Gain–2 and Proportional Gain–3, beginning with the 0 settings recommended for the instrument.
6. Perform a force calibration plot for the tip extracting and retracting at a z scan setting of 1 μm, set point = 0 volts, z-scan rate of 4–5 Hz, and *z* range to 1 μm. The tip deflection should read close 0.10 μm/div (*see* **Note 3**).
7. Open three separate channels for imaging the films in contact mode, such as channel 1, height; channel 2, deflection; and channel 3, friction. Set *x*/*y* range or scan size initially to 50 μm, and a *z* or height range to 10 nm.
8. Scan the film surface at a rate of 0.5–1 Hz (J scanner, 50–10 μm) or 2–10 Hz (E scanner 1 μm to 5 nm). The image in J scanner should appear as those shown in **Fig. 2A**. If no images appear at these settings and scanning method, adjust the integral and proportional gain in the software (*see* **Note 4**). These parameter set-

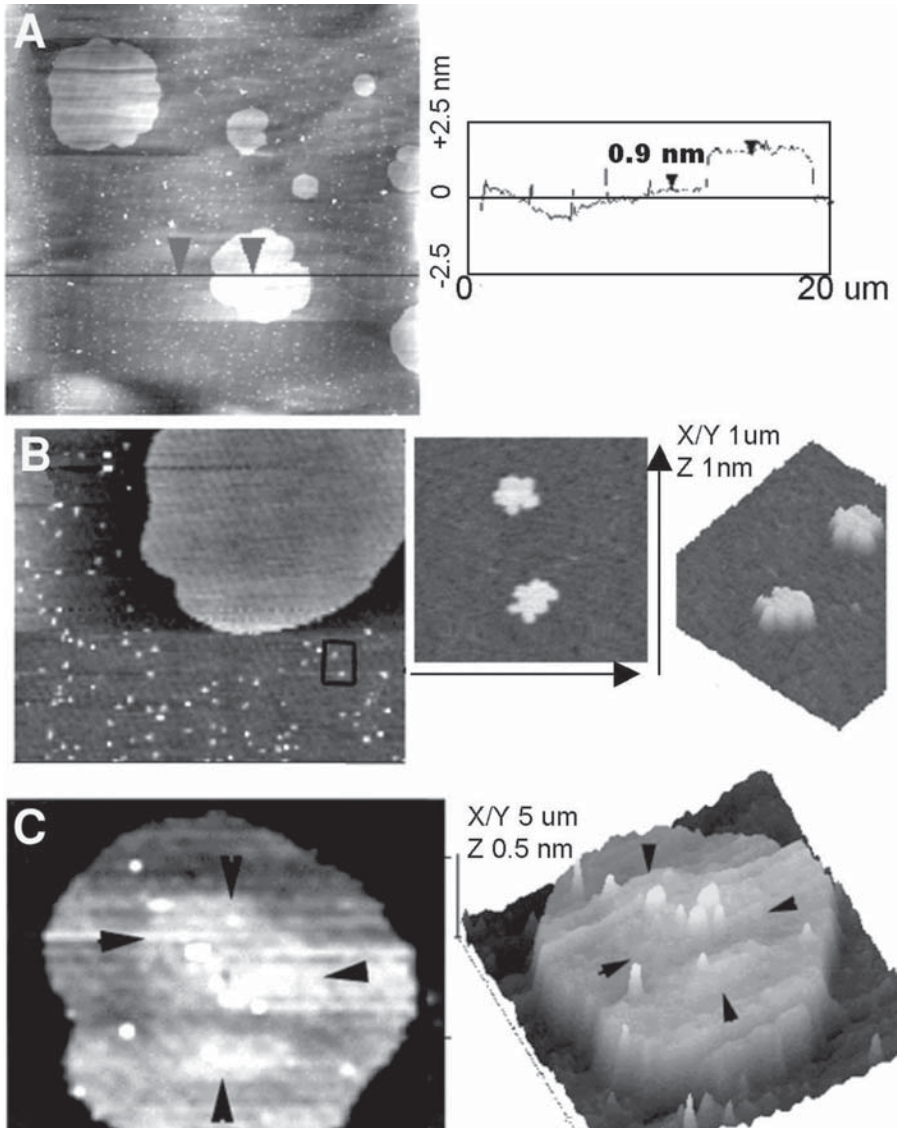

Fig. 2. AFM height mode images of solvent-spread BLES films deposited on mica. The line section analysis of the image in **(A)** suggests that the gel phase is 0.95 nm higher than the surrounding fluid phase, due to a different tilt of the phospholipid molecules in that phase compared with the fluid (*see* **Note 5**). The images in **(B)** shows that the fluid phase is not completely homogenous but has variety of micro-domains (<1 μm) as revealed by AFM and not seen in fluorescence (as in **Fig. 1B**). The gel domain **(C)** also has internal structures (region with arrows) and are possibly made with DPPC plus other saturated lipids of surfactant with differing chain lengths.

tings and methods can be found in further details in the nanoscope operation manual and has been discussed by others in details ***(13,21,22)***.

9. Save the first images and exact parameters used in files, and then zoom into various areas of the films. The zooming should be performed on the center of the condensed domains, in the fluid like phase, and at the edges of the gel-fluid regions, as shown in **Fig. 2B**. This can reveal various microstructures observed in such films beyond the gel and fluid like phase, such as smaller microstructures or domains (possibly surfactant proteins and protein–lipid aggregates) as shown in the right panel of **Fig. 2B**. The gel or condensed domains are not completely homogenous and show corrugation inside the domains as shown in **Fig. 2C**.

3.3. Structural Analysis and Interpretation of AFM Images

1. Change the setting of the software to off-line mode and choose the height mode image first.
2. The saved images in the height mode are then flattened. During flattening alter the z height between 10, 5, and 1 nm until the sharpest possible contrast between the gel and fluid phase is observed, as in **Fig 2A** the height was set to 5 nm.
3. Take a quick three-dimensional (3D) view of the image, and the gel-phase domains should be higher (brighter) than the fluid phase in such image (**Fig. 2C**).
4. Using the 2D flattened image perform a line section of the image in the vertical direction. The line should at least pass across a domain. The difference of this height between the gel and fluid phase should be around 0.8 to 1.3 nm. These height difference can reflect the molecular tilt of the phospholipids in the films (*see* **Note 5**) and are typical of the gel–fluid phase height differences as in other lipid films ***(7,14–16)***. For BLES films the height difference is about 1.3 nm and for DPPC films it is about 0.8 nm (**Figs. 1** and **3**).
5. In case of adsorbed films of rat surfactant (**Fig. 3A** and **B**) other regions of protein rich areas larger than gel or fluid domains are observed (shown by arrow). These domains are possibly adsorbed soluble proteins (**Fig. 3B**, the circular region), which has inserted into the monolayers, and interfere with the lipid pack-

---

Fig. 3. *(opposite page)* AFM height and deflection mode images of adsorbed films of (dys)functional surfactant from rat lungs. The image in **(A)** is from a film of normal rat (lung–lavage) surfactant and the one in **(B)** from the dysfunctional surfactant, in which the rat lungs underwent hyperventilation injury (*see* **Subheading 1.**) ***(18)***. The fluorescence microscopy images shown in the right side of each panel was obtained from the deposited films. The fluorescence image suggests that the edge of the gel domains (indicated by letter C in the images) in **(A)** are not smooth but contain different filamentous structure and microdomain (arrow) protruding from such domains as shown in the AFM. The large circular region or domain in **(B)** (arrow) is of different height and deflection profile compared to the fluid or gel phase, suggesting that these regions are possibly made of protein rich phase (since the estimates of soluble serum proteins in the dysfunctional surfactant was three times higher than those from normal surfactant ***[18]***).

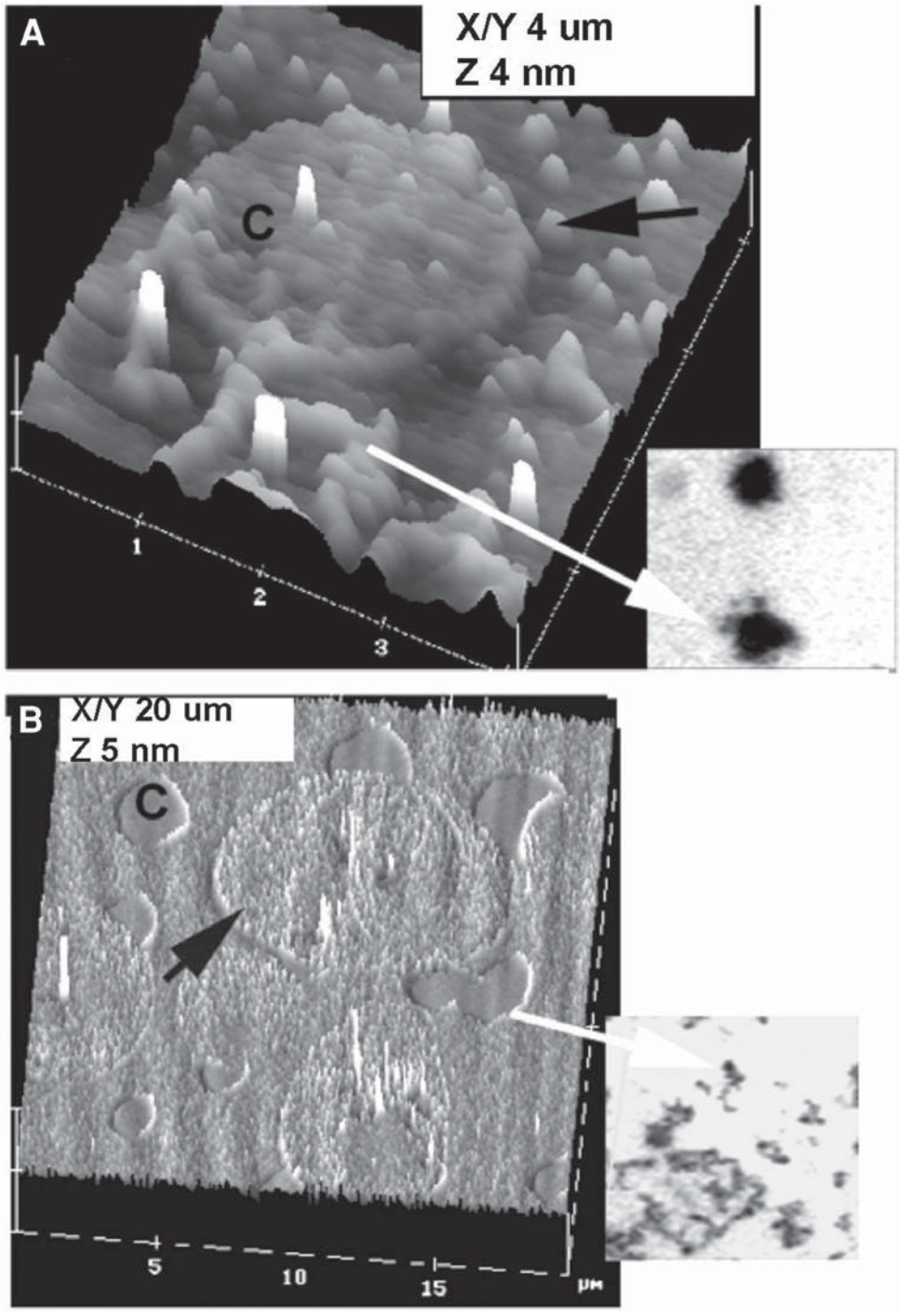
A
X/Y 4 um
Z 4 nm
C
1
2
3
B
X/Y 20 um
Z 5 nm
C
5
10
15
μm

ing. The effect of lipid packing efficacy can be monitored by measuring the gel domain diameters and height from normal vs dysfunctional surfactant films.

6. Because surfactant contains a host of other lipids and small amounts of hydrophobic proteins, various micro-heterogenous structures can be observed in the fluid-like phase. After selecting a heterogenous area, a 2D Spectral analysis using fast Fourier transform mode should be performed to observe any possible periodicity for these structures.
7. Save such analyzed images in a TIFF file (after the originals have been saved in the Nanoscope format) by exporting them for further display in normal image processing and display software for publication, image analysis and processing not supported by the AFM software. The AFM software normally allows for section analysis (line section, **Fig. 2A**), 2D Spectral and Grain size and fast Fourier transform analysis among others. Normally Adobe Photoshop, CorelDraw or NIH Imaging can allow further analysis and processing of the images.

4. Notes

1. For studies on interfacial film structures it is absolutely critical that a clean interface or water surface is maintained for all experiments. Although by doubly distilling (DDW) or deionizing the water using standard laboratory deionizers/distillation apparatus, it is possible to remove the inorganic components from water (resistivity ≈18 MΩ). However, we have observed certain surface-active (possibly organic) components enter the water during the distillation process or from the surrounding ambient laboratory environment. From our experience a second distillation of most laboratory distilled water using dilute potassium permanganate (0.01 m*M*) dissolved in this singly distilled water before the second distillation allows for quite high quality "clean" water interface. This can be easily monitored in a sensitive surface balance, by compressing the open surface of the DDW or so called "clean" interface and monitoring any change of surface tension or pressure at maximal compression or minimal surface area. Normally if there are any surface contaminants the surface pressure would increase by 2–5 mN/m at minimal surface area. At this stage, the surface can be cleaned by suction of the interface until the surface pressure drops to 0 mN/m. This clean surface is expanded further to the original surface area of the trough to 100%, and the film materials spread on this surface. Also a DPPC isotherm of a film on such a subphase, would show a sharp fluid to gel phase transition profile (*see* **Fig. 1A**) in the compression isotherm between 4–8 mN/m, if the DDW surface is clean. Surface contaminants tend to make the sharp transition more diffuse and sometimes may abolish them altogether, and can alter the typical size and shapes of the gel domains, by affecting the line tension of the gel–fluid domain boundaries ***(11,15)***.
2. It is still debated in the literature about the choice (pros and cons) of the best solid substrate to be used for film deposition for AFM ***(12,16)***. Both mica and glass surfaces are hydrophilic and therefore allow the polar regions of the films (or lipid head groups) to be deposited when they come in contact with either substrate. Although freshly cleaved mica is atomically flat and gives the best and

more accurate topographical profile of film structure at an sub-molecular resolution up to the atomic level ***(17)***, it does produce artifacts on film structures over time due to drying, since such films are scanned in air. Glass cover slips typically have surface heterogeneity (troughs and crevices) with depths exceeding 2–5 nm and therefore allow for a certain amount of the water to be trapped in the surface with the film during deposition ***(16)***. From our experience the glass substrate allows for imaging of such films for up to 3 days after deposit without any major changes of the gel or fluid domain structures of the films (as observed by fluorescence microscopy in **Fig. 1**). However the same films deposited on mica changes structure with an appearance of microstructures (smaller domains appearing in the fluid phase) within 2–-4 h of film deposit. Therefore depending on how quickly the films are scanned after deposit and the range of height resolutions required (<20 nm to >1 nm), glass or mica substrates should be chosen accordingly.

3. The parameters suggested here are the ones we use for scanning the films with our DI AFM. These can be altered depending on the instruments used; however, there are limits to how much force the tip can apply on the film before degrading the soft film structures. We find that the films can withstand forces ranging from 10 to 50 nN for imaging; however, others have used higher force >100 nN ***(16)***. Details of force–distance calibrations as applied to organic thin films have been discussed by others in details ***(12,13,22)***.
4. The imaging of the films using AFM depends only if the deposited films have the microstructures preserved as observed directly from the air–water interface using fluorescence microscopy (**Fig. 1A**). Other problems may occur if higher forces (<80 nN) are used during scanning, which can alter the film architecture and even remove the film from the area being scanned, by strong tip-film interactions. It is necessary therefore to image at least a DPPC film using fluorescence microscopy before and after deposit for preparing them for AFM imaging. The glass and mica slides containing the deposited film should be wiped on one surface for fluorescence imaging. Because the film deposits on both surfaces of the substrate, one of the surfaces (with film) should be cleaned by gently wiping this surface with a tissue paper or kim-wipe dipped in chloroform. This would remove the film from one surface and not allow for fluorescence from both surfaces to interfere during fluorescence imaging. From our experience we have noticed that many hours of AFM time is wasted in scanning a glass surface with broken or no films at all, since the fluorescence step was omitted. The fluorescent probe NBD-PC used below 1 mol% of the lipid do not significantly alter the film architecture, as confirmed at the air–water interface using lower-resolution Brewster angle microscopy, which do not require probe for imaging ***(8)***. If after using the fluorescence method, the AFM images cannot be observed, retract the tip from the surface and repeat procedure 6 through 9 (**Subheading 3.2.**) on a different region of the films.
5. The condensed or gel phase in BLES or DPPC films are formed as a result of the fatty acid chain being more perpendicular to the plane of the air–water interface compared to those in the fluid or expanded phase ***(23)***. This allows for the gel or

condensed phase to be imaged and the gel phase is considered as a tilt-condensed phase ***(11,23)***. However, AFM height differences between the gel–fluid phase do not give accurate numbers for the exact degree of tilt of the molecules in the gel compared with the fluid phase because the depression of the tip in a softer fluid phase varies depending on the composition of this phase. In case of BLES, a number of fluid phospholipid and surfactant proteins SP-B/C are present in the fluid phase (as determined from various model film studies ***[7,14]***). Therefore the exact degree of chain tilts are actually deduced using other techniques such as grazing angle incidence X-ray diffraction from such films ***(11)***. These results are in close agreement with AFM results obtained by line section of the domain boundaries (**Fig. 2A**). The AFM images in the friction mode can indicate regions of higher tip-surface interactions or the viscoelasticity of the gel or fluid phase, as suggested in the micro-heterogenous areas in Fig. 3B, with very small height differences observed in the deflection mode ***(15)***.

Acknowledgments

This work was supported by a collaborative health research grant from the National Scientific and Educational Research Council/Canadian Institute of Health Research (NSERC/CIHR). A.K.P. is a recipient of a Department of Science and Technology of India postdoctoral fellowship. We also gratefully acknowledge the valued advice and discussion of the data in this project with Dr. C. Yip, University of Toronto. K.N. is a CIHR-New Investigator at Memorial University.

References

1. Possmayer, F, Nag, K., Rodriguez, K., Quanbar, R., and S. Schürch (2001) Surface activity in vitro: Role of surfactant proteins. *Comp. Biochem. Physiol. A.* **129,** 209–320.
2. Nag, K, Munro, J. G., Hearn S. A., Rasmusson, J., Petersen N. O., and Possmayer, F. (1999) Correlated atomic force and transmission electron microscopy of nanotubular structures in pulmonary surfactant. *J. Struct. Biol.,* **126,** 1–15.
3. Goerke, J (1998) Pulmonary surfactant: Functions and molecular composition. *Biochim. Biophys. Acta* **1408,** 79–89.
4. Greise, M. (1999) Pulmonary surfactant in health and lung disease: State of the art. *Eur. Respir. J.* **13,** 1455–1476.
5. Veldhuizen, R. A. W., Nag, K, Orgeig, S., and Possmayer, F. (1998) The role of lipids in pulmonary surfactant. *Biochim. Biophys. Acta* **1408,** 90–108.
6. Nag, K, Perez-Gil, J., Ruano, M.L.F., Worthman, L. A. D., Stewart, J., Casals, C., and Keough, K. M. W. (1998) Phase transitions in films of lung surfactant at the air-water interface. *Biophys. J.* **74,** 2983–2995.
7. Von Nahmen, A., Schenk, M., Seiber, M., and Amrein, M. (1997) The structure of model surfactant as revealed by scanning force microscopy. *Biophys. J.* **72,** 463–469.

8. Piknova, B., Scheif, W.R., Vogel, V., Discher, B. M., and Hall, S. B. (2001) Discrepancy between phase behavior of lung surfactant phospholipids and the classical model of surfactant function. *Biophys. J.* **81,** 2172–2180.
9. Nag, K., Harbottle, R. R., and Panda, A. K. (2000) Molecular architecture of a self-assembled bio-interface: Lung surfactant. *J. Surface Sci. Technol.* **16,** 157–170.
10. Brockman, H. (1999) Lipid monolayers: why use half a membrane to characterize protein-membrane interactions? *Curr. Opin. Struct. Biol.* **9,** 438–443.
11. Kaganer, V.M, Möhwald, H, and Dutta, P. (1999) Structure and phase transition in Langmuir monolayers. *Rev. Mod. Phys.* **71,** 779–819.
12. Radmacher, M, Tillman, R.W., Fritz, M., and Gaub, H. E. (1992) From molecules to cells: Imaging soft samples with atomic force microscope. *Science* **257,** 1900–1905.
13. Zasadzinski, J. A. N., and Hansma, P. K. (1990) Scanning tunneling microscopy and atomic force microscopy of biological surfaces. *Ann. NY Acad. Sci.* **589,** 476–491.
14. Ding, J, Takamoto, D. Y, VonNahmen, A, Lipp, M.M., Lee, K.Y.C., Waring, A., and Zasadzinski, J. A. (2001) Effects of lung surfactant proteins, SP-B and SP-C and palmitic acid on monolayer stability. *Biophys. J.* **80,** 2262–2272.
15. Chi, L. F., Anders, F, Fuchs, H, Jhonston, R. R., and Ringsdorf., H. (1993) Domain structures in Langmuir-Blodgett films investigated by atomic force microscopy. *Science* **259,** 213–216.
16. Mikrut, J. M., Dutta, P., Ketterson, J. B., and MacDonald, R. C. (1993) Atomic-force and fluorescence microscopy of Langmuir–Blodgett monolayers pf 1,2,-dimyristoyl-phosphatidic acid. *Phys. Rev. B.* **48,** 14,479–14,487.
17. Zhai, X and Kleijn, J. M. (1997) Molecular structure of dipalmitoylphosphatidylcholine Langmuir–Blodgett monolayers studied by atomic force microscopy. *Thin Solid Films* **304,** 327–332.
18. Veldhuizen, R. A. W., Welk, B., Harbottle, R., Hearn, S., Nag, K., Petersen, N. O., and Possmayer, F (2001) Mechanical ventilation of isolated rat lungs changes the structure and biophysical properties of surfactant. *J. Appl. Physiol.* **92,** 1169–1175.
19. Nag, K, Perez-Gil, J., Cruz, A., Rich, N. H., and Keough, K. M. W. (1996) Spontaneous formation of interfacial lipid-protein monolayers from adsorption from vesicles. *Biophys. J.* **71,** 1356–1363.
20. Nag, K, Boland, C, Rich, N. H., and Keough, K.M.W. (1990) Design and construction of an epifluorescence microscopic surface balance for the study of lipid monolayer phase transition. *Rev. Sci. Instrum.* **61,** 3425–3430.
21. Gibson, C.T., Watson G. S., and Myhra, S. (1996) Scanning force microscopy-Callibrative procedures for "best practice." *Scanning* **19,** 564–581.
22. Gibson, C. T., Watson G. S., Mapledoram, L. D., Kondo, H., and Myhra, S. (1999) Characterization of organic thin films by atomic force microscopy:application of force vs distance analysis and other modes. *Appl. Surf. Sci.* **144/145,** 618–622.
23. Scheif, W. R., Touryan, L., Hall, S.B., and Vogel, V. (2000) Nanoscale topographic instabilities of a phospholipid monolayer. *J. Phys. Chem.* **104,** 7388–7393.